Research on Engineering Structures & Materials
www.jresm.org

Research Article

Large-scale in-situ infiltration and load testing on collapsible soils: A case study from Egypt's new administrative capital

Soha Emad Said [*,a], Yasser Moghazy El-Mossallamy [b], Hossam El-Din Ali [c], Ashraf Ahmed Reda El-Shamy [d]

Dept. of Geotechnical Engineering, Faculty of Civil Engineering, Ain Shams University, Cairo, Egypt

Article Info

Article History:

Received 30 Sep 2025

Accepted 02 Jan 2026

Keywords:

Collapsible soil;
In-situ testing;
Infiltration;
Problematic soils;
Partial saturation

Abstract

Collapsible soils are often challenging from a geotechnical standpoint and are found in many parts of the world. As urban development rapidly extends into Egypt's desert regions, construction projects increasingly encounter issues related to these problematic soils. In their natural dry state, collapsible soils tend to have relatively high strength. However, when inundated, they undergo major particle rearrangement and sudden volume reduction, which can cause serious structural issues like cracking, tilting, or even failure. In Egypt, sources of wetting might include irrigation of farmland, leaks from sewage systems, or occasional rainfall. This paper discusses a large-scale in-situ test that includes a deep infiltration system aimed at assessing the collapse potential and settlement behavior of collapsible soils at an arid site within Egypt's New Administrative Capital. The location, with its uneven terrain, required extensive cut-and-fill earthworks, with excavated materials reused as engineered fill. After observing excessive settlements that impacted a structure, two in-situ tests were carried out: one on original native soil and another on compacted fill. The tests showed that the native soil settled approximately 2 cm under collapse conditions, while the compacted fill experienced about 9 cm of settlement, indicating the high vulnerability of reworked sand–gravel materials to collapse.

1. Introduction

Collapsible soils are partially saturated loose-grained soils with low density that can withstand considerable stress in their natural unsaturated state, but upon wetting, these soils usually undergo a radical particle rearrangement accompanied by a decrease in volume [1, 2]. These soils are highly problematic and cover a vast area worldwide, thus requiring special consideration in geotechnical design to prevent potential significant financial losses due to structural damages [3]. The term "collapse" differs from primary settlement or consolidation as it occurs depending on the degree of wetting and has a significant uncontrolled magnitude [4]. At the natural water content, collapsible soil particles are held together by silt grains, capillary tension, silt and clay bonds, as well as cementation [1]. However, when the water content increases, the bond holding the soil particles together weakens or is completely washed, and the collapse mechanism is instigated due to the decrease in the shear strength and/or rearrangement of the soil particles [5,6]. Thus, causing noticeable uncontrolled settlement affecting the structures found upon it [7]. The uncontrolled settlement is mainly due to the non-uniform distribution of the percentage of bond particles within the soil, causing extreme bond sensitivity upon wetting. Another reason for the uncontrolled subsidence (differential settlement) is the unequal increase in soil water content beneath the same structure.

*Corresponding author: soha.emad@eng.asu.edu.eg
[a]orcid.org/0009-0004-7304-3033; [b]orcid.org/0009-0001-1446-3984; [c]orcid.org/0000-0001-7525-3393; [d]orcid.org/0000-0002-1605-7269
DOI: http://dx.doi.org/10.17515/resm2026-1204st0930rs

Collapsible soils exist in many locations across Egypt [8]. Geological data and research confirmed that the dry sand of the Egyptian deserts contains a percentage of fines that can cause potential collapse. Collapsible soils in Egypt are often formed by dried mudflows from rivers and flood streams in shallow water depths, leaving tiny air pockets in the soil voids [9, 10]. Collapsible soils cover huge areas in Siwa Oasis, the north delta, southwest Egypt, extending to North Sudan, the northwest coast of Egypt, along the Red Sea coast, Qattara depressions, and the coastal region of the Sinai Peninsula [11]. For newly developed cities in Egypt, collapsible soils are encountered and cause structural damage in many projects. These areas include 6th of October, 10th of Ramadan City, New Maadi, New Amereya, El Obour, Alex/Cairo desert highway road and Borg El-Arab in Alexandria [2, 12], as well as the huge New Administration Capital City in the south-east of the metropole city of Cairo.

The possible sources of soil wetting that may occur within the lifetime of the structure should be studied to take protective measures so that the structures can be found safely on these problematic soils. In Egypt, the main sources of wetting are mainly manmade, such as landscape irrigation, fracturing/leakage from water pipes or sewer lines [13]. Rainfall represents a small fraction of water sources in Egypt [12]. The non-uniformity of increased water content causes varying collapse potential, leading to a high risk of differential settlement and distortion angle in existing buildings [14]. It is important to classify collapsible soil based on severity with a quantifiable variable known as the collapse potential, CP or I_c, which represents the percentage of sudden volume loss when soil undergoes collapse, determined at any stress level [15]. Basic soil index properties and Atterberg limits can be used to form indirect correlations with the collapse potential. An empirical relation was suggested [16] to define the collapse potential with reference to the natural water content, w_{cn}, the degree of saturation, S_r, the plastic limit, PL, and the plasticity index, PI. Jennings and Knight [17] proposed a guideline for the type of soil, grain size distribution and critical degree of saturation.

Researchers [18, 19] also utilized standard penetration (SPT) values, cone penetration (CPT) tip resistance and seismic velocity to provide correlations with the collapse potential, but the results were rather poor. For preliminary identification of collapsible soils, the in-situ density was plotted against the liquid limit [20]. A detailed review of the different criteria and indirect methods to estimate collapse potential can be found in [11, 21]. These correlations are mostly for identification purposes only. For settlement estimation, laboratory or field tests should be performed to obtain quantitative data [22]. For fine grained soils, the collapse potential can be determined from laboratory oedometer tests, either single or double [17, 23]. However, for coarse gravelly soils, standard laboratory oedometer tests are unsuitable for capturing actual field-scale behaviour due to sample size limitations that are not representative of the in-situ conditions [24] and differences in collapse mechanisms [25]. Field settlements are consistently and significantly greater than laboratory predictions. This discrepancy is especially pronounced in complex, heterogeneous field conditions [26]. The traditional oedometer apparatus dimensions require modifications and design of a large-scale oedometer apparatus to capture the collapse mechanism of coarse grained gravelly soils [24, 26]. Attempts to capture the collapse settlement of sandy gravelly soils based on large-scale direct shear tests using artificial neural networks (ANN), multi-gene genetic programming (MGGP) and evolutionary polynomial regression (EPR models) are presented in [27-29].

Sensitivity classification criteria to judge the severity of foundation problems with reference to collapse potential were proposed in many publications [17], as well as a mathematical equation [30] to show the effect of relative compaction, RC, applied normal stress, and degree of saturation on the collapse potential. Other lab tests are occasionally conducted, such as triaxial test with suction control [31], suction-controlled oedometer tests using axis translation [32-35]. To obtain more realistic results that simulate the in-situ conditions, it is preferred to conduct field tests. Field tests can give more realistic results, especially in the case of gravelly soils where undisturbed samples cannot be gained even from open pits. However, limited research could be found considering field tests to determine the collapse potential [36-40]. The most effective methodology for testing soil collapsibility in the field is the in-situ collapse test (ISCP) [36], which is essentially a plate load test with larger dimensions to permit testing of a relatively large zone of the collapsible soil. The initial test was further modified [41] to account for the required normal stress acting on

the foundation. The test is conducted at natural water content conditions, and once the desired stress level is reached, water is added to the soil pit to increase the degree of saturation. The collapse potential can be determined by plotting the stress-settlement relationship from the obtained test data. In continuation, large-scale plate load tests were carried out in Greece to determine the collapse potential of collapsible soils at the subsurface [42]. Seismic dilatometer test [43] can also be utilized to determine the collapse potential. In this paper, a new large-scale in-situ test with a deep infiltration system is elaborated. This study addresses a critical gap in practice: the inability to rapidly assess the long-term, deep saturation collapse risk of foundations within a practical timeframe. While previous research has relied on shallow infiltration limited to subsurface saturation [2, 42, 44, 45], this work introduces a novel, integrated field methodology that accelerates deep saturation to simulate long-term performance in days rather than months or years. By simultaneously applying deep infiltration wells (10m depth) and surface ponding directly beneath a loaded, full-scale foundation pad, this study directly triggers and measures the full collapse mechanism that would otherwise develop slowly over years. This approach yields a major key advance by providing a definitive performance comparison proving that reworked engineering fill is significantly more vulnerable to collapse than native soil. The work thus provides a prescriptive, accelerated testing framework to prevent potential risks of foundation design in arid, collapsible deposits.

2. New Administration Capital City Case Study

2.1. General Site Description

The site location for the conducted large-scale tests was in the New Administration Capital City (NACC) in Egypt. This specific area was chosen as it exists in an arid and uninhabited region that is currently under urbanization and development. Geological studies show that the site is located within the Red Mountain formations in the Cairo-Suez district [46]. The natural soil at the studied site is composed of red to reddish brown, coarse to fine-grained gravel with varying amounts of fines and iron oxides.

A new residential compound containing villas, a services building and internal roads is under construction at the studied zone. Due to the mountain terrain, the natural topography had elevation differences of more than 10 meters. Before construction, earthworks (cut and fill) were conducted to reach the required architectural platform levels. The fill material consisted of recompacted native soil material obtained from the cut regions. The compacted engineering fill varied in thickness according to the location and reached a maximum value of about 10 meters. After completing most of the villas, significant cracks and settlement were observed in some buildings, which were attributed to water ingress from leakage of the temporary sewer tank located near the damaged villas. The observed settlement within one building ranged from 20 to 120 mm, along with tilting and severe cracks.

A primary assumption for the large settlement could be induced soil collapse due to infiltration of the sewage water below the foundation. A large-scale in-situ test was designed and conducted to determine the collapse potential of cut and fill areas at the site location.

2.2. Geophysics Investigation

A two-dimensional resistivity imaging survey was performed to investigate the project area. A total of three imaging profiles were surveyed and studied at different locations within the distressed zone to detect the presence of waterlogging in the soil subsurface layers, as shown in Fig. 1.

The conducted geophysical investigation has shown three separate zones of the subsoil that have different degrees of saturation. A sample for the 2-D geoelectrical resistivity imaging for Profile No. II (along points 4, 5 and 6) is shown in Fig. 2. These three zones were detected at different depths and different horizontal extensions along the three geophysical sections. The observed heterogeneity of the degree of saturation is due to the distance between the observed location and the source of water, as well as due to the soil heterogeneity regarding the amount and type of fines, and hence the hydraulic conductivity that affects the seepage paths.

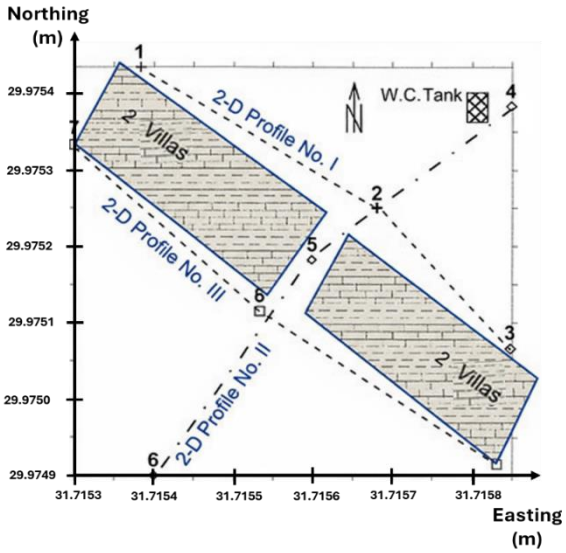

Fig. 1. Location map of the three imaging profiles

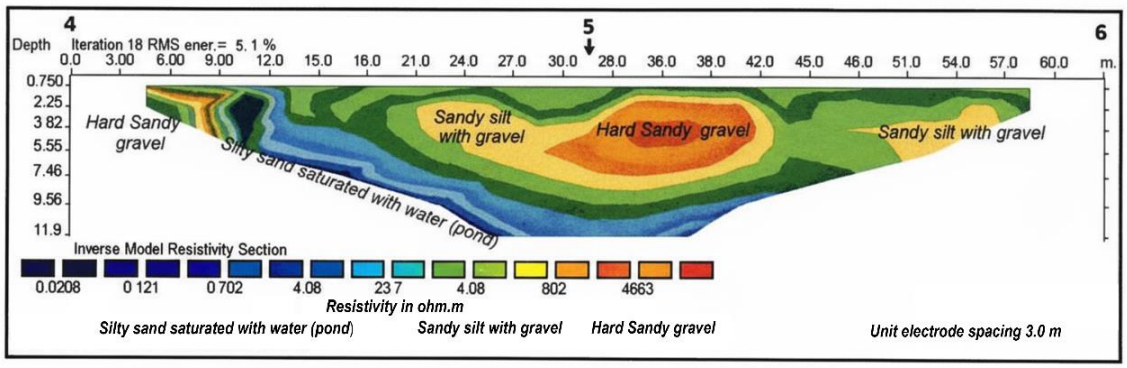

Fig. 2. Two- dimensional geoelectrical resistivity imaging for Profile No. II (along points 4, 5 and 6)

2.3. Site Investigation and Laboratory Tests

A total of 50 boreholes with a depth of 10 m from the ground surface were conducted during the initial site investigation to provide soil samples for lab testing. From the borehole results, no initial groundwater table was present. Sieve analysis results confirmed that the entire depth of the borehole consisted of sandy gravel with silt. The average percentage of fines in all soil samples varies between 11% and 19% (Fig. 3). The compaction state of the reworked engineering fill was determined using laboratory Modified Proctor tests, yielding an average optimum moisture content (OMC) of 6.5% and a maximum dry density (MDD) of 22.1 kN/m^3, shown in Fig. 4. Field quality control using sand cone tests confirmed in-situ dry densities corresponding to 90–95% of the Proctor MDD.

A summary of the soil index properties is presented in Table 1, while detailed test procedures are described in [47]. The soil consists of a coarse-grained skeleton (≈81% gravel and sand), forming a highly porous framework [48], with highly plastic fines (LL ≈ 86.3%, PI ≈ 43.9%) acting as a bonding agent under unsaturated conditions. At the low natural water content of the arid site, high matric suction maintains a strong but metastable structure. Collapse occurs when water infiltration reduces suction and weakens interparticle bonds, allowing particle rearrangement and densification. Previous studies indicate that reworked compacted soils are generally susceptible to collapse under appropriate loading and wetting conditions [35], with the initial degree of compaction being a controlling factor [49]. The in-situ dry density and natural water content indicate that the tested soil is dry of the optimum with a relative compaction of about 90%, thus highly susceptible to collapse [50, 51].

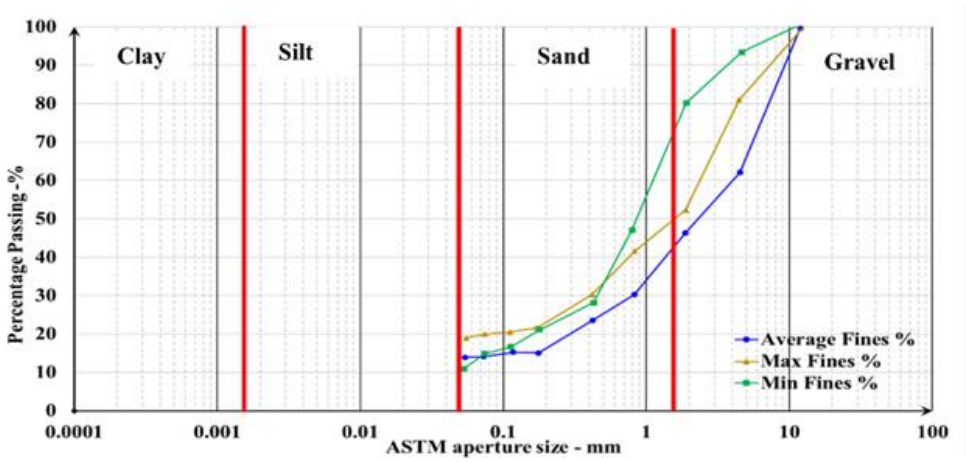

Fig. 3. Average sieve analysis for site location

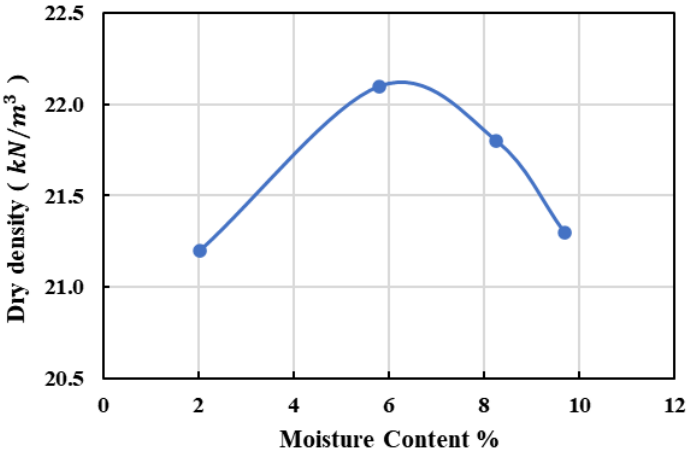

Fig. 4. Modified proctor compaction curve

Table 1. Summary of soil index properties

Property	Unit	Range	Average Value
Gravel	%	(51.0 - 60.0)	52.0
Sand	%	(15.0-39.0)	29.0
Fines	%	(10.0 – 25.0)	19.0
Specific Gravity (G_s)	---	(2.6 – 2.9)	2.8
Natural water content (w_c)	%	(1.0 - 2.5)	2.0
Dry Density (γ_d)	kN/m^3	(16.5 – 19.8)	19.0
Optimum Moisture Content (OMC)	%	(6.0 - 7.0)	6.5
Max. Dry Density (MDD)	kN/m^3	(20.0 -23.0)	22.0
Liquid Limit (LL)	%	(84.0 - 87.0)	86.3
Plastic Limit (PL)	%	(41.0 - 42.7)	42.4
Plasticity Index (PI)	%	(43.0 - 44.3)	43.9

In addition, to emphasize the severity of the issue, sieve analysis data was obtained from boreholes conducted with a depth of 30 m for other mega projects throughout the area of the NACC. The borehole logs indicated that cemented sand, sandy gravel and silty sand covered large areas in the NACC. For relevance, only data to a depth of 10m from the ground surface is presented. Fig. 5 shows a sample of the percentage of fines present in the specified soil layers. Fig. 6 shows a histogram of the fines' percentage distribution. From these two figures, the percentage of fines from the sample data ranges from about 4% to 50%. The probability of constructing foundation projects upon soil with 13% fines, the same average fine percentage in the studied area, is about 30%. Therefore, the risk of dealing with collapsible soils in the NACC is relatively high.

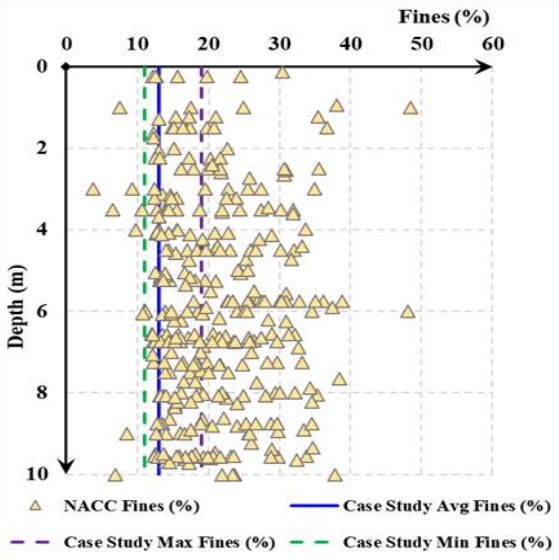

Fig. 5. Fines percentage throughout NACC and at the case study location

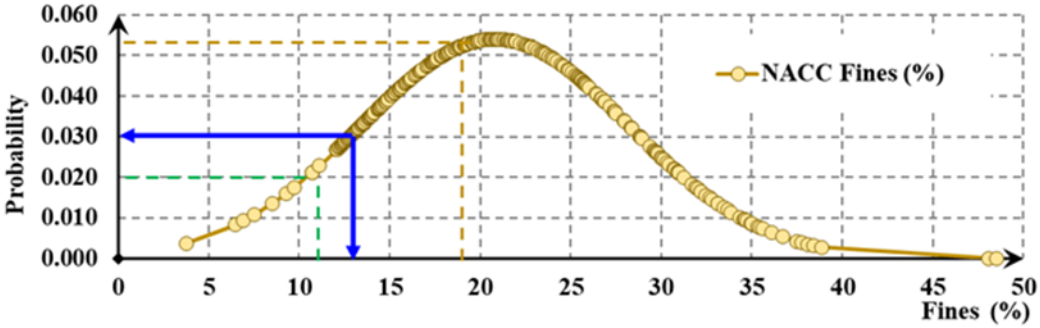

Fig. 6. Statistical analysis of fines percentage from NACC sample data

2.4. Static Plate Load Tests (SPLT)

Before the execution of the large-scale in-situ test, static plate load tests (SPLTs) were performed. A total of five tests, with a plate diameter of 50 cm, were carried out on the reworked engineering fill material in the zone surrounding the damaged villa to study the reason for the severe observed damage. Fig. 7 shows the settlement values under constant load in the dry state and at the end of inundation. The settlement values vary significantly, not only at the end of the wetting process, but in the dry state for each tested sample, indicating that the soil is rather heterogeneous.

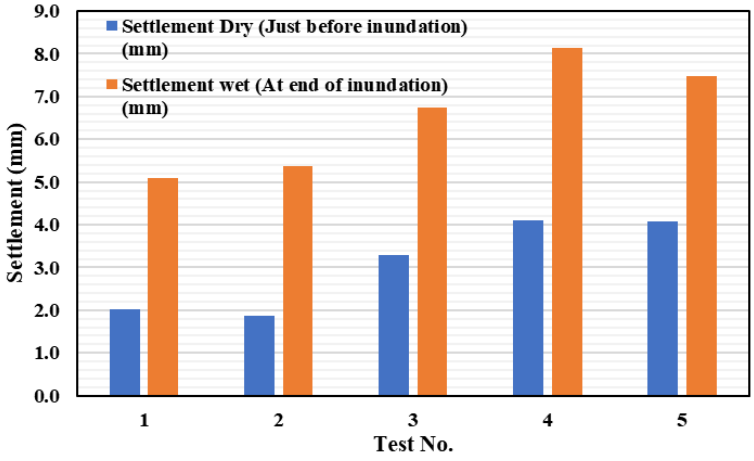

Fig. 7. SPLT Settlement values at constant load just before and at the end of inundation

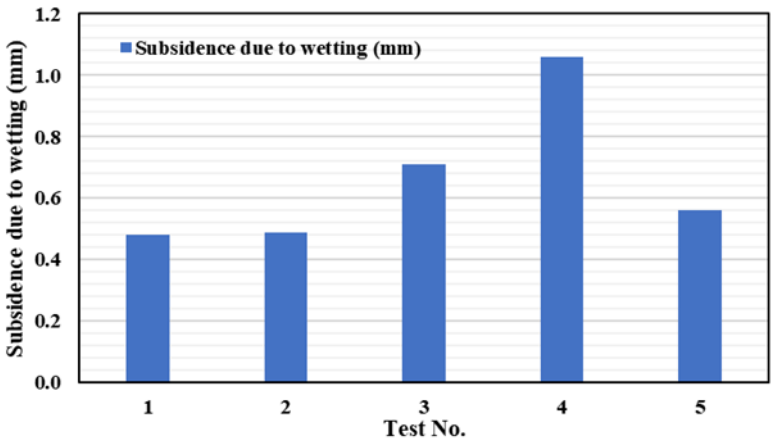

Fig. 8. Sudden subsidence at constant load due to water only from SPLT

The measured settlement values after wetting do not explain the collapse mechanism, as the time is limited to some hours, and hence the water has not penetrated the whole thickness of the collapsible layer. The sudden subsidence (difference between settlement values just before and just after inundation) under constant load for all tests is shown in Fig. 8. The percentage of increase in settlement due to wetting ranges from 13% to 26%. These values approve the high soil heterogeneity and hence its high sensitivity to wetting. Therefore, large-scale in-situ tests were performed to get a better understanding of the problem.

3. Large-Scale In-Situ Test

3.1. Test Setup

The setup for the proposed large-scale in-situ test consisted of 2 main aspects: a loading system and a wetting system. The wetting system was subdivided into subsurface wetting and deep infiltration. The importance of the deep infiltration system was to accelerate the soaking of the relatively thick fill layer (≈10 m), which is highly sensitive to small increases in water content depending on fines content and compaction degree. Five wells, approximately 9 m deep, were drilled at the start of the test setup, as shown in Fig. 9. These wells were equipped with perforated PVC pipes connected to a water tank via a valve to control the amount of water being fed to the system. Then the test location was prepped for the installation of the subsurface water feeding system, which consisted of horizontal perforated pipes in a filter layer connected to the same water tank via a separate valve, as shown in Fig. 10.

(a) (b)

Fig. 9. Deep infiltration system (a) Schematic (b) Photograph

To ensure the pipes remained unaffected by settlement, they were overlain with a thin layer of sand, as shown in Fig. 11. After the completion of the wetting system, preparation for the loading system began. The loading system consisted of a reinforced square concrete footing with dimensions (2 m x 2 m x 0.4 m), which was poured above the subsurface layer, as shown in Fig. 12.

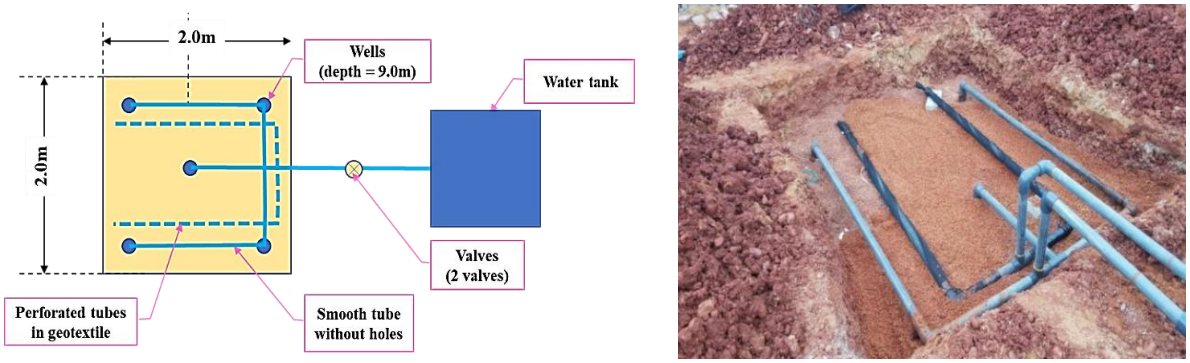

(a) (b)

Fig. 10. Subsurface wetting system (a) Schematic (b) Photograph

Fig. 11. A thin sand layer to prevent the settlement of pipes

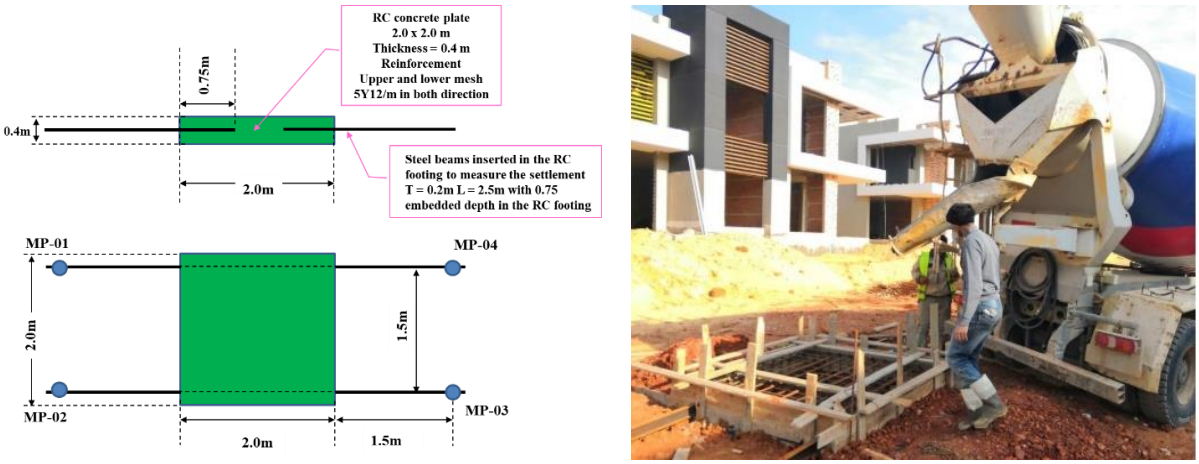

(a) (b)

Fig. 12. Construction of RC footing (a) Schematic (b) Photograph

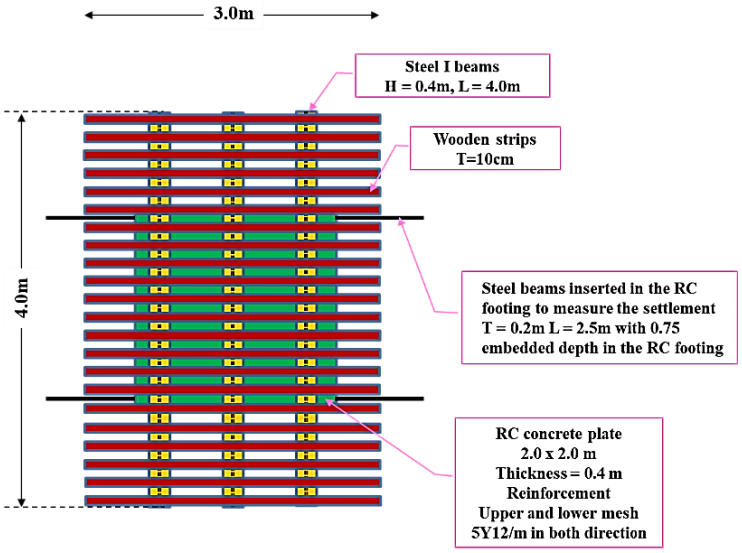

Fig. 13. Plan for the loading system

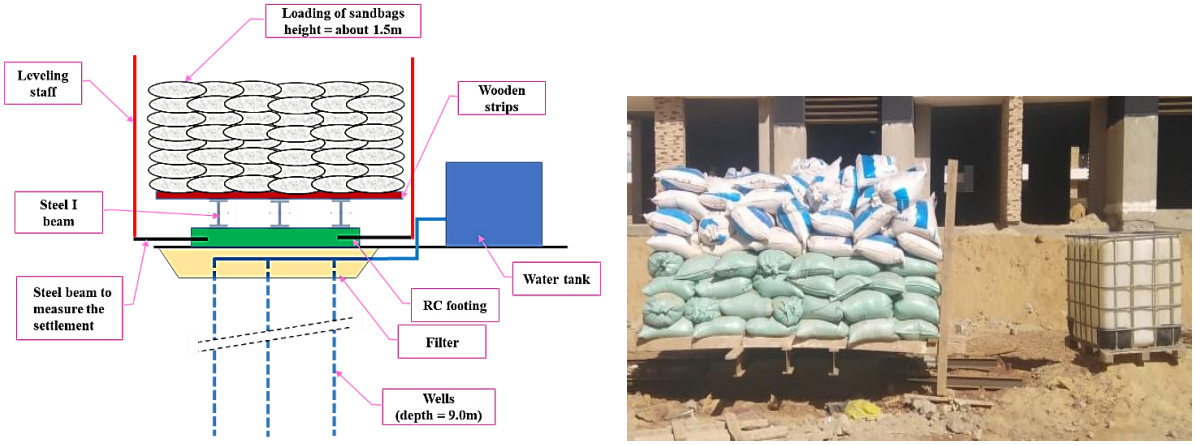

(a) (b)

Fig. 14. Final test setup (a) Schematic (b) Photograph

The applied stress was approximately 100 kPa to simulate the foundation's allowable stresses. Steel beams were embedded in the RC footing with an anchorage length of 0.75 m to act as a guideline when measuring the settlement. Then, a (3 m x 4 m) platform, as shown in Fig. 13, consisting of equally spaced wooden strips with a thickness of 0.1 m, was constructed above the RC footing. The platform was supported by steel I-beams with a height of 0.4 m and a length equal to 4 m. Finally, sandbags with a height of about 1.5 m were loaded onto the platform. Fig.14 shows the final test setup.

3.2. Test Procedure

The previously described large-scale in-situ test was set up at two locations: one at a cut zone and one at a fill zone near the building with a reported 12 cm settlement value. Settlement readings were taken at various milestones with reference to points MP-01, MP-02, MP-03 and MP-04 shown on the layout depicted in Fig. 12a. The process for the settlement readings is shown in Fig. 15. Vertical settlements at the four reference points (MP-01, MP-02, MP-03, and MP-04) were monitored manually using precise engineering leveling. All readings were referenced to a stable benchmark system located outside the zone of influence of the test. Initial readings for the settlement were taken seven days after pouring the RC footing, just before loading with sandbags, and just after finishing loading with sandbags. Then the watering system was opened, and settlement readings were also recorded.

A controlled infiltration test was conducted to saturate the soil beneath the RC footing extending to the entire depth of the constructed deep wells. The process was meticulously monitored by recording the time and amount of infiltrated water at each stage. The infiltration process was monitored continuously. Approximate saturation was determined based on the field observations regarding the cessation of rapid infiltration and the establishment of sustained surface ponding for a period of at least 3 hours. The methodology for confirming approximate saturation through controlled flooding and observable field indicators is consistent with established practices for large-scale collapsible soil testing [2]. Settlement readings continued periodically every day for 2 weeks after the infiltration process began until the rate of settlement reached less than about 1 mm/10 days. The obtained results were used to plot the time-settlement relation.

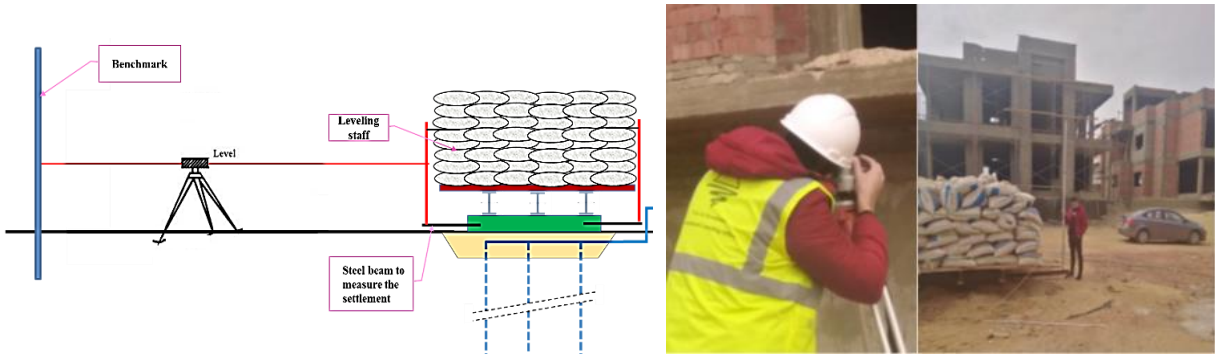

(a) (b)

Fig. 15. Settlement measurements process (a) Schematic (b) Photograph

4. Results and Discussion

4.1. Fill Zone (Recompacted Backfill)

For the fill zone, the baseline settlement values were taken on (Day 0), seven days after pouring the RC plate, which was also the start of loading with the sandbags, indicated by station 1 in Fig. 16. At milestone 2 (Day 13), just after finishing loading with the sandbags, the average relative settlement for the four reference points MP-01, MP-02, MP-03 and MP-04 was 10 mm. On Day 19, the soaking process began, Milestone 3, and the settlement values were recorded just before and just after the water valve was opened. Fig. 16 shows a substantial increase in the settlement values upon wetting, which was expected as a typical behavior of collapsible soils. These results indicate that despite the controlled field test conditions, equal water feeding and symmetric loading process, significant settlement variation occurred within the 4 points of the (2×2) m plate.

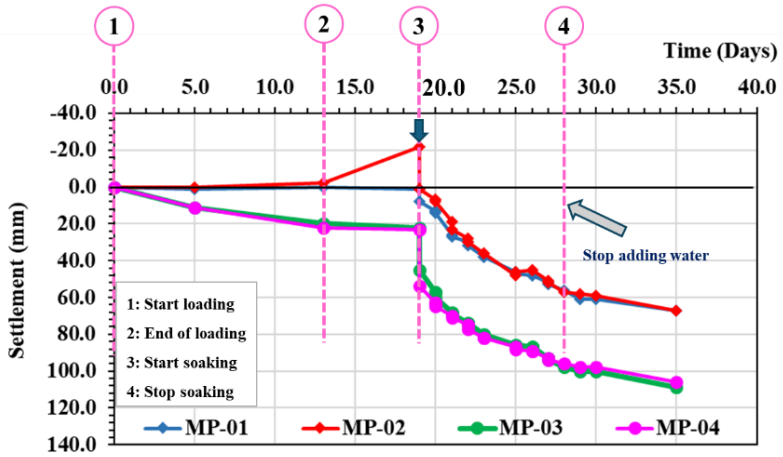

Fig. 16. Time vs. settlement curve for recompacted backfill zone for the four reference points : MP-01, MP-02, MP-03 and MP-04

Therefore, the structure of the cemented sandy gravel soil and the bond material result in an unequal effect on the settlement values upon wetting and lead to nonhomogeneous performance. Between Milestone 2 and Milestone 3, Point MP-02 experienced upward movement due to the slight rotation of the concrete plate resulting from the non-uniform settlement within the small footing. On Day 28, the soaking system was turned off due to concerns about its effect on surrounding structures, as 35 m^3 of water had been used without reaching full saturation (convergence was not reached). Nonetheless, readings continued until Day 35. The maximum total settlement recorded was 67 mm for MP-01 and MP-02, 109 mm for MP-03 and 106 mm for MP-04. The average total settlement was 87.2 mm.

4.2. Cut Zone (Native Soil)

The same process applied to the fill zone was performed on the cut zone (Native Soil) with Day 0 as the baseline for the settlement readings, taken seven days after pouring the RC plate. The loading of the concrete plate started on the same day, as shown in Fig. 17. At the end of the loading period, indicated by Milestone 2 in Fig. 17, the average relative settlement was about 4 mm. At constant load, the settlement continued to increase, and readings were taken. On Day 20, the wetting system was activated, and readings were taken just before and just after the start of the wetting process. Readings were taken every day afterwards until Day 31, where the average relative settlement reached a value of 21 mm. Only 6 m^3 of water was required to reach the fully saturated state (convergence was reached).

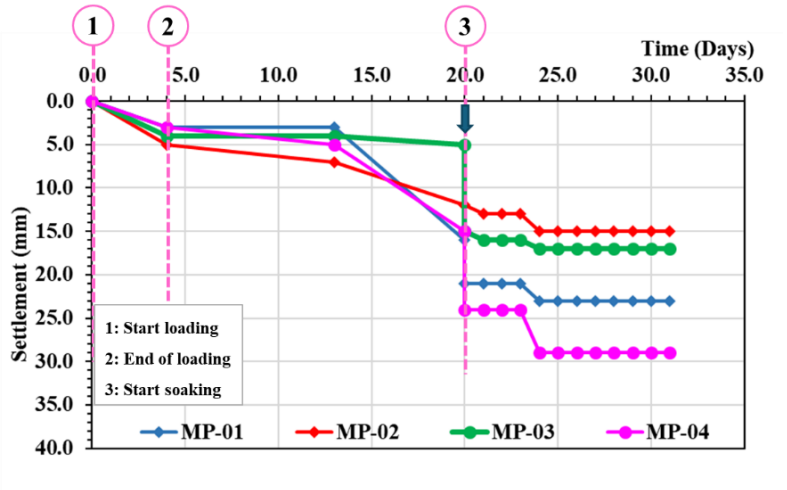

Fig. 17. Time vs. settlement curve for cut (native) zone for the four reference points : MP-01, MP-02, MP-03 and MP-04

4.3. Comparison between Native Soil and Reworked Backfill Zones

4.3.1 Infiltration Rate

The combined subsurface and deep infiltration system aimed to achieve a near-saturated condition, indicated by a constant infiltration rate and stabilization of settlement. The progression of infiltration rates with time for the native soil and reworked backfill zones is shown in Fig. 18, while the corresponding accumulative absorbed water is presented in Fig. 19.

In the native soil zone, upon applying the wetting system, rapid infiltration ($2m^3$/day) was exhibited, reflecting initial pore water absorption. Crucially, the rate of absorbed water decreased until infiltration ceased on the third day, resulting in immediate surface ponding, recorded as fully saturated. This behavior is indicated in Fig. 18 by the transition to zero infiltration rate. This persistent inability to infiltrate additional water over three consecutive days is direct field evidence that the soil's field capacity was exceeded, and a state of approximate saturation was achieved (after approximately 3 m^3 of applied water), shown in Fig. 19, and maintained within the influence zone of the tested area. The water volume applied after ponding began was 3 m^3, ensuring that the saturated condition was pervasive. The low permeability observed upon saturation is attributed to the high fines content, where the mobilized fines migrate, partially infilling the inter-particle voids

and reducing permeability. Therefore, in native soil a smear zone with low permeability was developed around each well preventing water flow and affecting the performance of native soils outside the smear zones.

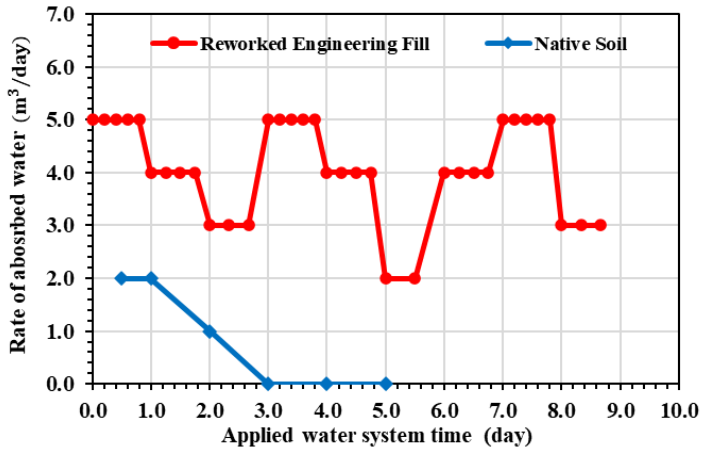

Fig. 18. Rate of absorbed water with time for both the native soil and reworked backfill zones

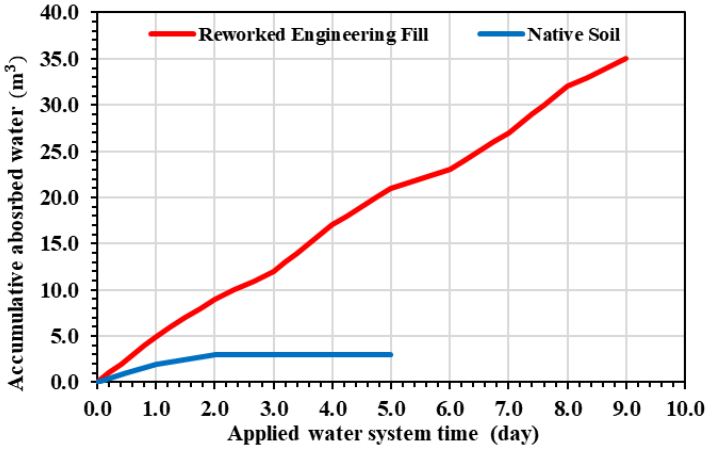

Fig. 19. Applied water system time vs. accumulative absorbed water for both the native soil and reworked backfill zones

In contrast, the reworked engineering fill zone exhibited variable but consistently finite infiltration rates throughout the test, never reaching a state of full saturation or ponding, despite applying a total water volume of 35 m^3. This behavior demonstrates the dynamics of unsaturated flow in the reworked soil deposit. The highly variable infiltration rates, shown in Fig. 18 and expressed as variable slopes in Fig. 19, are a direct signature of soil heterogeneity as well as the repeated cycle of smear zone development (where soil is remolded to a lower permeability) and degradation by infiltrating water. This key difference in hydrological response is critical for interpreting the subsequent load test results.

4.3.2 Time-Settlement Relations

The average time-settlement curves for both the cut (native) and fill cases were plotted on the same graph, as shown in Fig. 20. For the fill zone, the upward movement values were neglected, and the settlement curve was extrapolated from Day 13 to Day 19, the start of the infiltration process. From the graph below, it can be noticed that for the native soil zone, the settlement performance with time due to water infiltration is stabilized, and convergence values are observed. The average additional measured settlement due to soaking is about 8 mm. However, for the fill zone, the settlement performance with time due to water infiltration has not stabilized, and the settlement kept increasing with time even after the water valve was closed on Day 28. The average additional settlement due to soaking is about 80 mm.

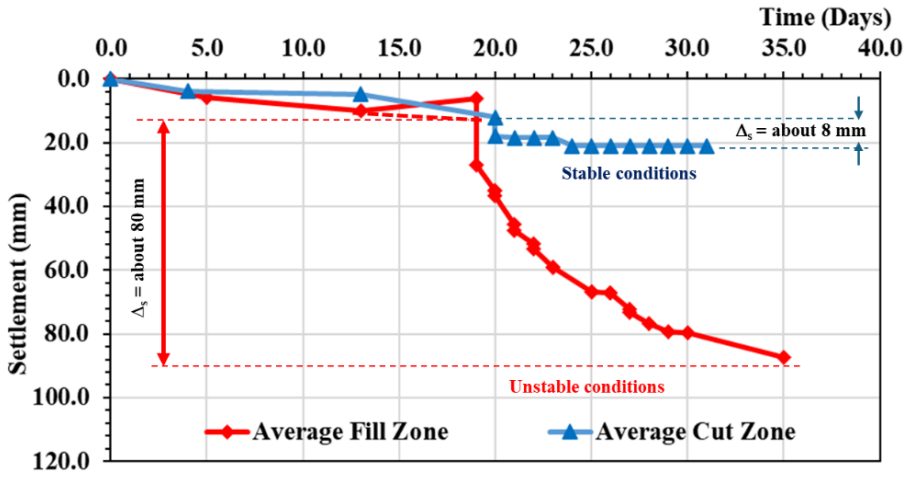

Fig. 20. Comparison between average settlement vs. time curve for native and fill zones

4.3.3 Settlement and Serviceability Criteria

A comparison between settlement and angular distortion values at different loading stages for native and engineering fill zones is shown in Table 2. The initial coordinates of the four reference points (MP-01, MP-02, MP-03 and MP-04) with respect to the center of the RC footing is shown in Fig. 21. Due to the rigidity of the RC footing, the angular distortion values are obtained from the overall rotation caused by average differential settlement between opposite edges. According to estimated average angular distortion values, there is a very high risk for structural damage according to allowable serviceability limit states [52], since β is greater than 1:300.

Table 2. Comparison between settlement and angular distortion values at different loading stages for native and reworked compacted backfill zones

Item	Case	Unit	Native Soil	Engineering Fill
Average Settlement	Just Before Wetting	mm	10.00	12.00
	After Completion of Wetting Process	mm	23.00	86.50
	Percentage of Increase	%	130.00	620.83
Average Angular Distortion (β)	Just Before Wetting	---	1:350	1:90
	After Completion of Wetting Process	---	1:280	1:95

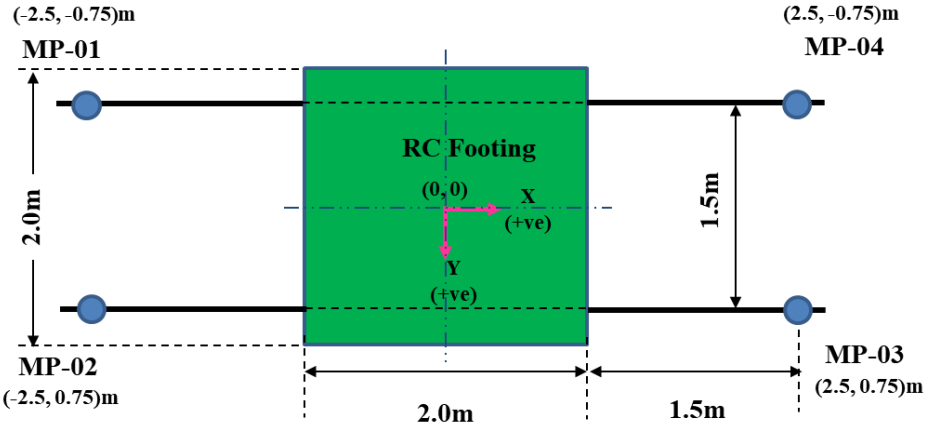

Fig. 21. The initial coordinates of the four reference points with respect to the center of the RC footing for settlement and angular distortion measurements

Table 2 shows that at the dry stage (before starting the wetting process), the average settlement is rather identical for both native as well as reworked compacted soil. The slight difference in behavior is believed to be attributed to the compaction process. Both the native soil and the reworked compacted backfill exhibit collapse upon wetting; however, the collapse potential of the reworked backfill is at least four times greater than that of the native soil. This marked difference is attributed to the disturbance and destruction of the native soil's naturally developed honeycomb fabric, which evolved over geological time. Reworking and recompacting using a vibratory smooth roller disrupt this metastable structure and creates a denser yet more water-sensitive fabric, thereby significantly increasing susceptibility to wetting-induced collapse.

4.3.4 Uncertainty Treatment and its Effect on Engineering Conclusions

Settlement was measured using precise engineering levelling with a vertical accuracy of ±1.0 mm per reading. Instrument calibration, temperature corrections, balanced sight lengths, and early-morning observations were employed to minimize systematic and environmental errors. Measurement uncertainty was propagated through successive elevation differences, resulting in an estimated uncertainty of ±1.5 mm for differential settlement between monitoring points, which directly affects the angular distortion values. For a measured differential settlement of 15 mm over a 1.5 m foundation edge, the calculated angular distortion is 1/100. However, the actual differential settlement could be as low as 13.5 mm or as high as 16.5 mm due to measurement uncertainty (15mm ±1.5mm). This translates to a possible angular distortion range of approximately 1/111 to 1/91. The uncertainty ranges (confidence intervals) were considered in the interpretation of settlement–time curves and angular distortion calculations, confirming that the observed deformation trends exceed measurement noise. Consequently, measurement uncertainty does not affect the engineering conclusions regarding serviceability performance.

4.3.5 Numerical Simulation

The large-scale in-situ tests were simulated in Plaxis 3D 2024.1 [53] by implementing the Barcelona Basic Model (BBM) [54] to capture the unsaturated and collapse behavior. The 3D model consisted of 10-noded elements with a maximum, minimum and average mesh element size of 6m, 0.14m and 2m respectively, with a refined zone beneath the foundation and surrounding the deep well to ensure accuracy in the high-stress region. The geometry was designed to be sufficiently large to minimize boundary effects (35 x 35 x 20) m. The boundary conditions were normally fixed along the X and Y axes, fully fixed at the bottom (Zmin) and free at the top (Zmax). The geometry of the models is shown in Fig. 22, whereas the BBM parameters are shown in Table 3. In the BBM, a single set of parameters defines the soil for both wet and dry conditions, as the main feature of the BBM is the possibility to account for a smooth transition from a partially saturated to a fully saturated state [53]. The performance at a certain degree of saturation is controlled by the soil water characteristic curve (SWCC). The estimated SWCC for sandy gravel with void ratio = 0.5 and specific gravity = 2.80 is shown in Fig. 23 based on data from literature [55].

Table 3. Barcelona Basic Model (BBM) parameters for native soil and reworked engineering fill

Symbol	Unit	Description	Native Soil	Reworked Engineering Fill
ν'	---	Poisson's ratio	0.2000	0.2000
κ	---	Slope of the swelling line in (v-ln p') plane	0.0010	0.0020
λ	---	Slope of the compression line at full saturation in (v- ln p') plane	0.0043	0.0190
κ_s	---	Slope of the swelling line in (v-ln s) plane	0.0006	0.0018
k_s	---	Tensile strength due to suction	0.1000	0.1000
ϕ	degree	Friction angle at critical state	38.0000	38.0000
e_0	---	Initial void ratio	0.5000	0.5000
p_r	kPa	Reference effective pressure	2.0000	2.0000
r	---	Soil stiffness with suction	0.5000	0.3000
β	kPa^{-1}	Rate of increase of soil stiffness with suction	0.0100	0.0200
α	---	Coefficient of the plastic potential	0.4600	0.4600

The settlement values just before and after completion of the wetting process from the Plaxis simulations are plotted against the actual in-situ values for both native and reworked engineering backfill with an error bandwidth of ±10%, shown in Fig. 24. The model simulations show very good agreement with the in-situ settlement values with R^2 (coefficient of determination) =0.99, MAE (mean absolute error) =1.58 mm and RMSE (root mean square error) =1.80 mm, indicating that the implemented model is capable of capturing the actual behavior and can be used to predict expected settlement in the design stage for future projects.

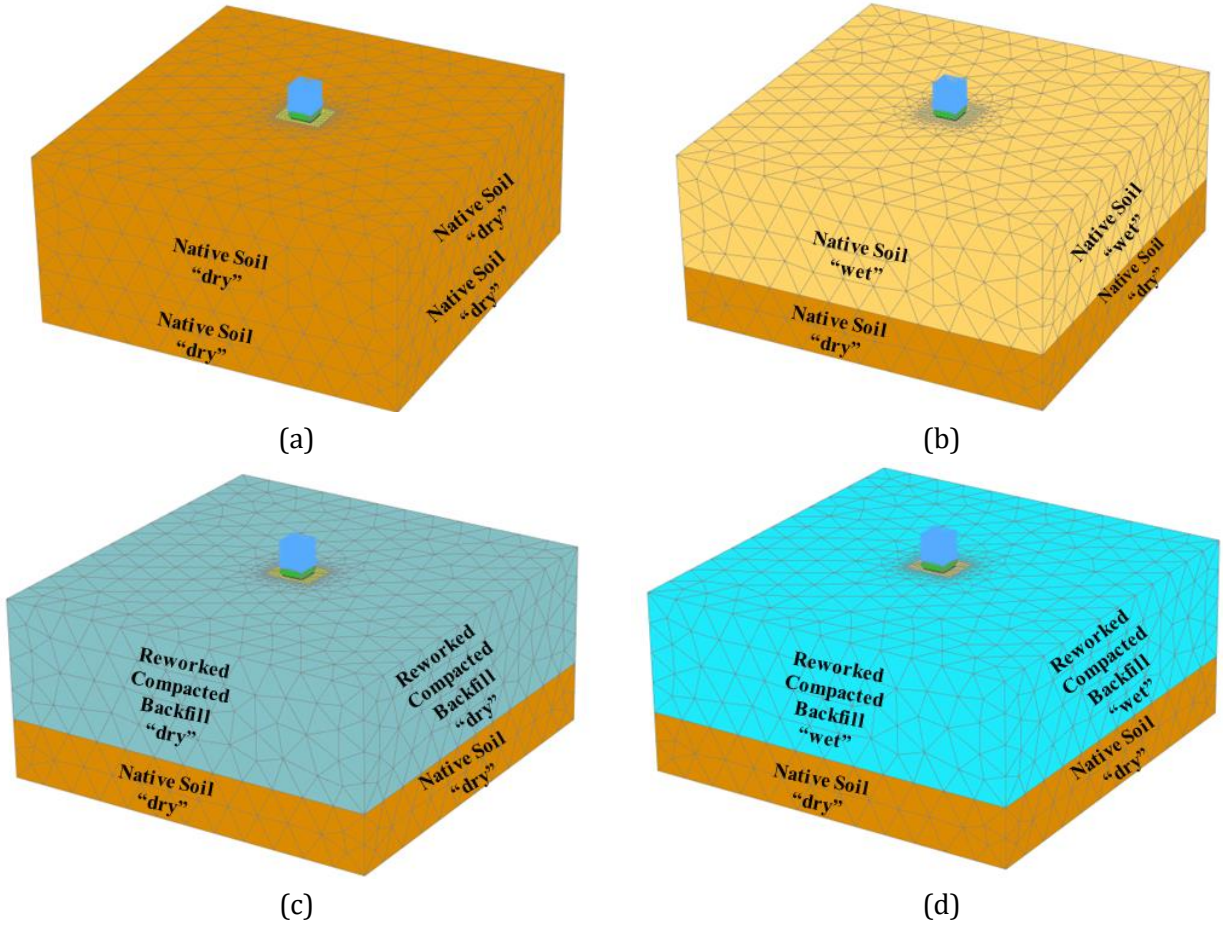

Fig. 22. Plaxis 3D model simulations for (a) Native soil dry (b) Native soil wet (c) Reworked backfill dry (d) Reworked backfill wet

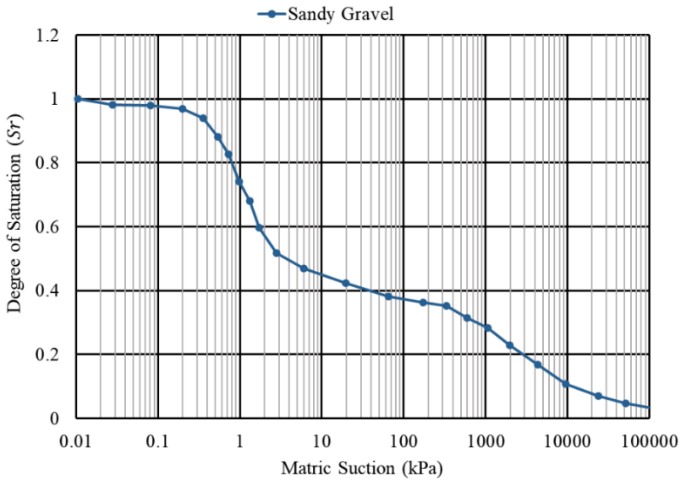

Fig. 23. Soil water characteristic curve "SWCC" for Sandy Gravel (void ratio = 0.5, specific gravity = 2.80)

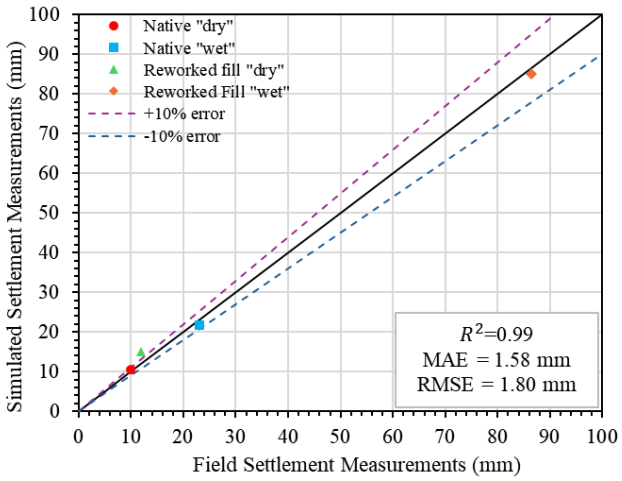

Fig. 24. In-situ and simulated settlement values for native soil and reworked engineering backfill

4.3.6 Scope and Limitations of the Numerical Analysis

The numerical analysis presented is a simplified, phenomenological back-analysis, not a predictive model. Its sole purpose is to demonstrate that the magnitude of the measured field collapse can be reproduced using reasonable soil parameters and a constitutive model for unsaturated soil. A formal mesh study and comprehensive sensitivity analysis were not performed. Parameters were derived from standard correlations, literature values, and iterative manual calibration to fit the load-settlement data. The high R^2 value is thus interpreted as evidence that the model can adequately replicate the observed collapse settlement, not as validation of a perfect or predictive unsaturated soil model.

4.4. Comparison Between SPLT And Large-Scale In-Situ Load Test

A comparison between the average settlement values from the SPLT and large-scale in situ test for the reworked compacted backfill zone is shown in Table 4. From the results, under constant load in the dry state, a scaling factor of about 4.0 can be assumed to account for the dimensions of the loading plate, stress influence zones and nonlinear strain distributions. The observed settlement ratio of approximately 4:1 between the large-scale RC footing and the SPLT is presented as an empirical, site-specific outcome rather than a generic scaling law.

On applying the scaling factor, both tests give relatively equivalent settlement results in the dry state. However, upon wetting, the values between the two tests differ drastically. This is due to the saturation area and testing period. For the SPLT, the saturation area is limited to the subsurface, and the test is conducted within a few hours. For the large-scale test, deep wells were used to infiltrate the water into the soil at greater depths up to 9 m, and the test was conducted for a minimum of 30 days. Fig. 16 shows that the reworked compacted backfill zone took almost 35 days to reach the maximum measured settlement as given in Table 2, and yet stable conditions were not obtained. The influence depth of a surface load is theoretically limited, often approximated as smaller than 2B to 4B (where B is the foundation width) [56]. For the 0.5m SPLT plate, this corresponds to an influence depth of 1-2 m and about 4-8 m for the 2.0m RC footing. However, there is no influence depth for the effect of wetting. Collapse behaviour is a volumetric strain triggered by wetting, which is mostly independent of the applied footing stress and its influence depth depends on the depth of the collapsible soil and the amount and rate of water infiltration. At identical stress conditions, the collapse settlement from the SPLT is governed by a small soil volume just beneath the plate that will be fully saturated and develops a smear zone that prevents further water infiltration, whereas in reality, collapse settlement is governed by a much greater volume, encompassing the wetted zone, shown in Fig. 25. The time as well as the source of water in the reality play decisive actions on the soil performance that cannot be simulated via the simple static plate loading test. Furthermore, to normalize the results, the average field collapse strain, ε_{cf}, is calculated by dividing the collapse settlement by the stress influence depth for both cases, which

yields 0.4% and 2.2% for the SPLT and large-scale in-situ test respectively. Thus, further validating that the SPLT cannot fully capture the expected collapse mechanism upon deep infiltration.

Table 4. Comparison between SPLT and large-scale in-situ test for reworked compacted backfill zone

Item		Unit	SPLT	Large-Scale in-situ Test
Average Settlement	Just Before Wetting	mm	3.07	12
	After Completion of Wetting Process	mm	6.56	86.5
	Percentage of Increase	%	113.75	620.83

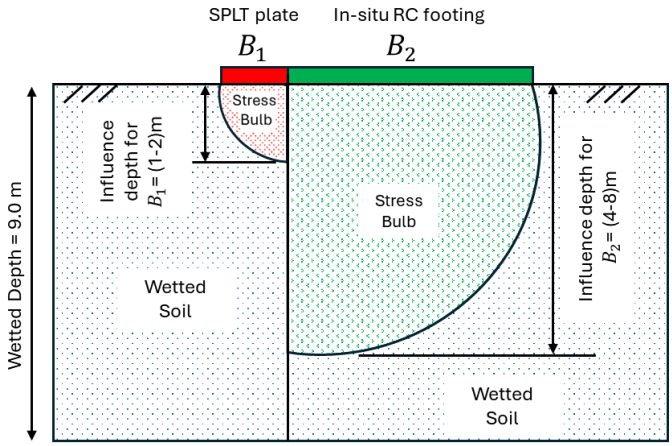

Fig. 25. Comparison between influence depth and stress bulb for applied load on SPLT plate (B1) and in-situ RC footing (B2)

5. Conclusions

From the conducted large-scale in-situ tests with a water infiltration system on both cut and fill zones, the following conclusions can be drawn:

- The performance of the native soil in the cut zone differs drastically from that of the compacted backfilled soil, despite using the cut material for the fill zone. The destruction of the bonded joints of the native soil is the reason for this large difference between the performance of native and recompacted soils.
- The amount of clay, compaction methodology, compaction energy and degree of compaction have a great effect on the performance of fill soils used as engineered fill.
- Static plate load tests cannot accurately predict the expected increase in settlement due to water ingress in collapsible soil. It can only indicate the risk of collapsibility of the used compaction material.
- Settlement due to applied foundation stress is affected by the footing dimensions (influence depth); however, there is no exact influence depth for the effect of water ingress. The effect of water ingress is a time phenomenon that depends on the soil type, percentage and type of fines, initial water content, source of water and quantity of seeped water as well as the depth of the collapsible soil layer.
- The accelerated deep infiltration system demonstrates the severe collapse potential inherent in the soil fabric by rapidly triggering the wetting-induced settlement mechanism. In the large-scale test on reworked fill, this resulted in approximately 11 cm of settlement within days. Importantly, the magnitude of this settlement is comparable to the 10–12 cm of damage-causing settlement observed over a year in a nearby villa affected by subsurface leakage. While the timescales differ, both cases confirm that the ultimate collapse potential of the soil is sufficient to produce structurally damaging settlements. Thus, the test provides

a validated lower-bound estimate of the geotechnical risk posed by prolonged moisture ingress in this arid environment.

- Additional measures to control the risk of soil collapse by water ingress are to apply isolation systems combined with a subsurface drainage system for all green areas, swimming pools and utilities such as sewer and irrigation pipes to prevent water infiltration into soil susceptible to collapse, which may cause severe cracks and settlement in nearby structures.
- Non-uniform infiltration of water due to leakage can cause differential settlement and distortion of structures that can lead to severe damage.
- Identification and classification of collapse behavior from in-situ tests and settlement recordings indicate that the average angular distortion values can exceed allowable serviceability limit states. There is a very high risk for structures founded on such soil type.
- The novelty of this approach lies in wetting not only the subsurface during testing, which is the case in most previous studies but also using deep wells to ensure the wetting of the soil at greater depths to simulate realistic foundation long term conditions.
- The results of conventional static plate loading test with inundation give only indication on the soil sensitivity in case of water ingress. Further work to correlate the test results with the expected long-term performance is needed.
- The different infiltration behaviors observed between the native and reworked engineering fill soils warrant a cautious interpretation. For future recommendations, it is important to note three key limitations in the presented dataset that should be addressed for a definitive mechanistic explanation: hydraulic conductivity measurements, quantitative reference to seepage pathways and grain-size-specific microstructural interpretation.

References

[1] Knodel PC. Characteristics and problems of collapsible soils. US Department of the Interior, Bureau of Reclamation, Denver Office, Research and Laboratory Services Division, Materials Engineering Branch; 1992.

[2] Ali NA. Practical engineering behavior of Egyptian collapsible soils, laboratory and in-situ experimental study. Open Journal of Civil Engineering. 2021; 11(3): 290 - 300. https://doi.org/10.4236/ojce.2021.113017

[3] Mebarki M, Benyahia S, Dahmani S. Laboratory improvement of clay mineralogical and swelling properties using hydraulic binder treatment. Research on Engineering Structures and Materials. 2025; 11: 933 - 55. https://doi.org/10.17515/resm2025-752ma0313rs

[4] Rogers CD. Types and distribution of collapsible soils. In Genesis and properties of collapsible soils 1995 Apr (pp. 1-17). Dordrecht: Springer Netherlands.

[5] Ali N, Metwally M, El Sawwaf M, Nazir A. Study the correlation between microstructural features and geotechnical properties of collapsing soil at elevated temperatures. Geoenergy Science and Engineering. 2024; 238: 212923. https://doi.org/10.1016/j.geoen.2024.212923

[6] Abdulwadood HW, Albusoda BS. The Collapsible Soil Definition and Mitigation Strategies: A Review Study. Journal of Engineering, 2024; 30(11): 142 - 63. https://doi.org/10.31026/j.eng.2024.11.09

[7] Almahbobi S. Experimental study of volume change and shear strength behaviour of statically compacted collapsible soil, PhD Dissertation, Cardiff University, 2018.

[8] Sakr M, Mashhour M, Hanna A. Egyptian collapsible soils and their improvement. Proceedings of GeoCongress 2008: Geosustainability and Geohazard Mitigation, New Orleans, Louisiana, 2008. https://doi.org/10.1061/40971(310)81

[9] Ali NA. Performance of partially replaced collapsible soil–Field study. Alexandria Engineering Journal. 2015; 54(3): 527-32. https://doi.org/10.1016/j.aej.2015.05.002

[10] El Mosallamy M, Abd El Fattah TT, El Khouly M. Experimental study on the determination of small strain-shear modulus of loess soil. Hbrc Journal. 2016; 12(2): 181-90. https://doi.org/10.1016/j.hbrcj.2014.11.010

[11] Ayadat T, Hanna AM. Assessment of soil collapse prediction methods. Int J Eng Trans B Appl. 2012; 25(1): 19 – 26. https://doi.org/10.5829/idosi.ije.2012.25.01b.03

[12] Gaaver KE. Geotechnical properties of Egyptian collapsible soils. Alexandria Engineering Journal. 2012; 51(3): 205 – 10. https://doi.org/10.1016/j.aej.2012.05.002

[13] Cui YJ, Delage P. Soil Collapse due to Water Infiltration. Environmental Geomechanics. 2013: 149 - 69. https://doi.org/10.1002/9781118619834.ch6

[14] Hamdy DB. Origin and characteristics of collapsible soils state of the art report. Innovative Infrastructure Solutions. 2024; 9(10): 401. https://doi.org/10.1007/s41062-024-01673-5

[15] D5333-03 ASTM. Standard Test Method for Measurement of Collapse Potential of Soils. 1996.
[16] Feda J. Structural stability of subsident loess soil from Praha-Dejvice. Engineering Geology. 1966; 1(3): 201 – 19. https://doi.org/10.1016/0013-7952(66)90032-9
[17] Jennings JE, Knight K. A guide to construction on or with materials exhibiting additional settlement due to '"collapse"' of grain structure. Proceedings of Sixth regional conference for Africa on SMFE, 99–105, 1975.
[18] Lollo JA, Rodrigues RA, Elis VR, Prado R. Use of electrical resistivity to identify collapsible soils in Brazil. Bull Eng Geol Environ. 2011; 70(2): 299–307. https://doi.org/10.1007/s10064-011-0357-8
[19] Lollo JA, Vivanco JM., Curtis JS. Collapse susceptibility mapping using SRTM data obtained from Topodata Project. Eng Geol Soc Territ. 2015; 5: 885 – 91.
[20] Gibbs HJ, Bara JP. Predicting surface subsidence from basic soil tests. US Department of the Interior, Bureau of Reclamation, Division of Engineering Laboratories; 1962.
[21] Al-Rawas AA. State-of-the-art-review of collapsible soils. Sultan Qaboos University Journal For Science. 2000; 5(2): 115 - 35. https://doi.org/10.24200/squjs.vol5iss0pp115-135
[22] Houston SL, Houston WN, Zapata CE, Lawrence C. Geotechnical engineering practice for collapsible soils. Geotechnical & Geological Engineering. 2001; 19(3): 333 - 55. https://doi.org/10.1007/978-94-015-9775-3_6
[23] Abelev YM. Fundamentals of Design and Construction on Macroporous Soils. Stroivoenmorizdat, Moscow. 1948.
[24] Ng AM, Yeung AT, Lee PK, Tham LG. Design, fabrication, and assembly of a large oedometer. Geotechnical Testing Journal. 2006; 29(4): 298 - 305. https://doi.org/10.1520/GTJ100454
[25] Brink GE. The identification and characterisation of collapsible soils: a brief review of current practice. Proceedings of the 21st NZGS Symposium, Dunedin, New Zealand, 2021.
[26] Mokhtari M, Shariatmadari N, Heshmati R AA, Salehzadeh H. Design and fabrication of a large-scale oedometer. Journal of Central South University. 2015; 22(3): 931 - 6. https://doi.org/10.1007/s11771-015-2603-x
[27] Soleimani S, Jiao P, Rajaei S, Forsati R. A new approach for prediction of collapse settlement of sandy gravel soils. Engineering with Computers. 2018; 34(1): 15 - 24. https://doi.org/10.1007/s00366-017-0517-y
[28] Hasanzadehshooiili H, Mahinroosta R, Lakirouhani A, Oshtaghi V. Using artificial neural network (ANN) in prediction of collapse settlements of sandy gravels. Arabian Journal of Geosciences. 2014; 7(6): 2303 - 14. https://doi.org/10.1007/s12517-013-0858-9
[29] Ghanizadeh AR, Delaram A, Fakharian P, Armaghani DJ. Developing predictive models of collapse settlement and coefficient of stress release of sandy-gravel soil via evolutionary polynomial regression. Applied Sciences. 2022; 12(19): 9986. https://doi.org/10.3390/app12199986
[30] De Zoysa CJ, Dushan AK, Kurukulasuriya LC. Collapsibility Characteristics of a Residual Soil in Matale District, Sri Lanka. In ICSBE 2020: Proceedings of the 11th International Conference on Sustainable Built Environment, Singapore 13-22, 2021. https://doi.org/10.1007/978-981-16-4412-2_2
[31] Sun DA, Sheng DC. Collapse Behavior of Unsaturated Compacted Soils. In Advances in unsaturated soil, seepage, and environmental geotechnics, 102-110, 2006. https://doi.org/10.1061/40860(192)9
[32] Hilf JW. A investigations of pore-water pressure in compacted cohesive soils, Ph.D Disertation, University of Colorodo, 1956.
[33] Barden L, McGown A, Collins K. The collapse mechanism in partly saturated soil. Engineering Geology. 1973; 7(1): 49 - 60. https://doi.org/10.1016/0013-7952(73)90006-9
[34] Vilar OM, Rodrigues RA. Collapse behavior of soil in a Brazilian region affected by a rising water table. Canadian Geotechnical Journal. 2011; 48(2): 226 - 33. https://doi.org/10.1139/T10-065
[35] Opukumo AW, Davie CT, Glendinning S, Oborie E. A review of the identification methods and types of collapsible soils. Journal of Engineering and Applied Science. 2022; 69(1): 17. https://doi.org/10.1186/s44147-021-00064-2
[36] Mahmoud HH. The development of an in situ collapse testing system for collapsible soils, Ph.D Dissertation, Arizona State University, 1991.
[37] Krutov VI, Tarasova IV. A method for determining the magnitude of the" initial pressure" for slumping soils. Soil Mechanics and Foundation Engineering. 1964; 1(1): 12-7. https://doi.org/10.1007/BF01704025
[38] Macfarlane RB. A field test for detecting collapse susceptible soils, MSc. Dissertation, The University of Arizona, Arizona, 1989.
[39] Krutov VI, Éiduk RP. Determination of the relative slumpability of a soil by static probing from an exploratory-trench bed. Soil Mechanics and Foundation Engineering. 1971; 8(3): 172-4. https://doi.org/10.1007/BF01705109
[40] Bowers MT. IN SITU SOIL TESTING SYSTEM FOR COLLAPSIBLE SOILS (SETTLEMENT, COLLAPSE, ARIZONA), Ph.D Dissertation, Arizona State University, Arizona, 1986.

[41] Mahmoud HH, Houston WN, Houston SL. Apparatus and procedure for an in situ collapse test. Geotechnical Testing Journal. 1995; 18(4): 431 - 40. https://doi.org/10.1520/GTJ11018J
[42] Platis A, Malliou K. Large-Scale Plate Load Tests to Determine the Collapse Potential at Santorini 150 kV GIS Substation Site. In E3S Web of Conferences, Vol. 382, p. 12006, 2023. https://doi.org/10.1051/e3sconf/202338212006
[43] Rocha BP, de Carvalho Rodrigues AL, Rodrigues RA, Giacheti HL. Using a seismic dilatometer to identify collapsible soils. International Journal of Civil Engineering. 2022; 20(7): 857-67. https://doi.org/10.1007/s40999-021-00687-9
[44] Romero S, Ferreira DM, Fucale S. Evaluation of the collapsibility of soils in the semiarid region of Pernambuco, Brazil. The Scientific World Journal. 2014; 8(10): 1285–92. https://doi.org/10.17265/1934-7359/2014.10.010
[45] Bandeira AP, de Souza Neto JB, Coutinho RQ, Xavier JM, Chaves AM, da Silva Alves VL. Investigating the Collapsible Behavior of Sedimentary Soil in Shallow Foundations. Geotechnical and Geological Engineering. 2024; 42(4): 2725 - 43. https://doi.org/10.1007/s10706-023-02701-4
[46] Sallam E, Issawi B, Osman R. Stratigraphy, facies, and depositional environments of the Paleogene sediments in Cairo–Suez district, Egypt. Arabian Journal of Geosciences. 2015; 8(4): 1939 - 64. https://doi.org/10.1007/s12517-014-1360-8
[47] Tuleun L Z, Wasiu J. Mechanical behavior of silty-clayey lateritic soil stabilized with recycled municipal solid waste ash. Res. Eng. Struct. Mater., 2025; 11(3): 1121-1138. https://doi.org/10.17515/resm2024.204me0303rs
[48] Sun S, Zhu D, Zhang Z. Experimental study on the compression characteristics of sandy soil under impact loading. Research on Engineering Structures and Materials. 2025; 11(2): 903-920. https://doi.org/10.17515/resm2025-586me1223rs
[49] Bakhshandeh F, Noorzad R, Ta'negonbadi B. Experimental investigation of the properties of collapsible soil stabilized by colloidal silica. Scientific Reports. 2025; 15(1): 30032. https://doi.org/10.1038/s41598-025-15965-y
[50] Vilar OM, Rodrigues RA. Revisiting classical methods to identify collapsible soils. Soils and Rocks. 2015; 38(3): 265 - 78. https://doi.org/10.28927/SR.383265
[51] Silveira IA, Giacheti HL, Rocha BP, Rodrigues RA, Paulo S. Collapsible behaviour of a compacted lateritic sandy soil. Proceedings of the 7th International Conference on Geotechnical and Geophysical Site Characterization (ISC'7), 18–21, 2024.
[52] Skempton AW, MacDonald DH. The allowable settlements of buildings. Proceedings of the Institution of Civil Engineers, 5(6):727-68, 1956.
[53] Plaxis 2023.1. User Defined Soil Model-Barcelona Basic Model. 2023; 1–58.
[54] Alonso EE, Gens A, Josa A. A constitutive model for partially saturated soils. Géotechnique. 1990; 40(3): 405 - 30. https://doi.org/10.1680/geot.1990.40.3.405
[55] Li X, Li JH, Zhang LM. Predicting bimodal soil–water characteristic curves and permeability functions using physically based parameters. Computers and geotechnics. 2014; 57: 85-96. https://doi.org/10.1016/j.compgeo.2014.01.004
[56] Shahien M, Farouk A, Elgarf AM. Simplified Model for Determining the Depth of Influence below Surface Loaded Areas. Proceedings of the 18th Regional African Conference on Soil Mechanics and Geotechnical Engineering. Algeria, 2024.